Approximating Clustered Millimeter Wave Vehicular Channels by Sparse Subband Fitting

Thomas Blazek*, Erich Zöchmann*†‡, and Christoph F. Mecklenbräuker*
†Christian Doppler Laboratory for Dependable Wireless Connectivity for the Society in Motion
*Institute of Telecommunications, TU Wien, Austria
‡Department of Radio Electronics, TU Brno, Czech Republic

***Abstract*—Understanding millimeter wave (mmWave) vehicular channels is crucial for the application of mmWave technologies in vehicle-to-anything settings. However, as of yet, few attempts of low-complexity approximation of such channels exist. Prior results have shown that such channels are often composed of clustered multipath components, and this work builds on those results. We present an approach to project a measured mmWave channel into subbands. Sufficiently narrow subbands do not resolve the cluster structures and are efficiently approximated as sparse channels. We thereby render sparse tapped delay line model fits possible. In this contribution, we optimize sparse fits in subbands, and then combine all fits to approximate the full band. We evaluate this approach using vehicular mmWave channel measurements, and demonstrate that subband fitting results in efficient leveraging of sparse structures of mmWave channel data.**

***Index Terms*—mmWave, Vehicular Channel Models, c-LASSO, Cluster**

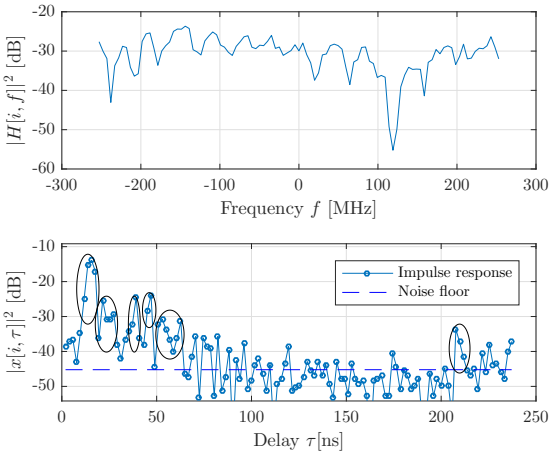

Fig. 1. Example transfer function and impulse response snapshot from measurements. Clusters are circled.

I. Introduction

As part of the 5th generation (5G) of mobile telephony, millimeter wave (mmWave) communications is expected to augment current technologies with additional wide-bandwidth communication channels. The current vehicular communications standards struggle to be implemented on the road. 5G mmWave offers new potential use cases [1] for vehicular communications. However, the vehicular channel is known to be challenging due to nonstationarity [2], and many of these challenges are exacerbated due to the high carrier frequency. Thus, accurate channel models are required for assessment of the capabilities and limits of vehicular mmWave applications.

To this end, mmWave channel measurements have been conducted, both indoors [3]–[5] and for outdoors vehicular channels. [6]–[8]. These measurements frequently demonstrate a cluster structure in the impulse response. Such a behavior was first documented at lower frequency band by [9], and can be frequently seen in wireless channels. Similar results were demonstrated in [10]. There, the authors did not try to exploit the structure, but merely documented it. Their results do however show, that while many multipaths are seen in mmWave channels, they can be clustered in a small number of scattering clusters, resulting in a cluster-sparse structure. This has been use by the authors of [11] through applying sparse methods to identify cluster positions for indoor measurements in the frequency range of $2-8$ GHz.

In this paper, we present an approach to approximate mmWave vehicular channel measurement with a cluster-sparse estimate. To achieve this, we project our signal of interest on a small frequency subband, which compresses the power contained within clusters, and apply the complex Least Absolute Shrinkage and Selection Operator (c-LASSO) to identify the cluster locations [12]. We then apply the derived algorithm to vehicular mmWave channel measurements for evaluation. Our results show that projecting on sufficiently narrow subbands ensures that the sparse estimation is able to identify the clusters, and by doing fits for parallel subbands, the channel can be approximated with high accuracy.

II. Channel Approximation

In this section, we propose a LASSO algorithm operating on subbands to accurately fit clustered channel data. We consider a wireless multipath channel that consists of a small number of K_0 clusters, each consisting of an known amount n_k of multipath components. The time-

variant impulse response of such channel can be written as

$$x[i,\tau] = \sum_{k=1}^{K_0} \sum_{j=0}^{n_k} x_{k,j}[i]\delta(\tau - \tau_k[i] - j) \tag{1}$$

Here, each of the K_0 clusters is assigned n_k taps, a cluster delay τ_k, and each tap is assigned a complex coefficient $x_{k,j}$. The index i denotes absolute time, while τ denotes the delay. Figure 1 shows a snapshot from the measurement campaign where these clusters are marked in the impulse response. We observe a N-point frequency snapshot $\mathbf{H}[i]$ that is a result of the Discrete Fourier Transform (DFT) of $\mathbf{x}[i]$, and is furthermore corrupted by noise

$$\mathbf{H}[i] = \mathbf{F}\mathbf{x}[i] + \mathbf{n}[i]. \tag{2}$$

Here, $\mathbf{F}$ is the centered, unitary DFT, we do not possess knowledge about the noise distribution. Furthermore, $\mathbf{x}[i]$ is a N-dimensional vector representation of the impulse response at time i with exactly $n_k \times K_0$ nonzero entries.

Given the structure in Equation (1), if the observed bandwidth were reduced by a factor of n_k, then the cluster taps would not be resolvable anymore, and the delay line would only show K_0 taps. Then, the multipaths would show up as small-scale fading. We will now exploit this by splitting the full measured bandwidth in P subbands. Every subband is then assigned its own delay line $\mathbf{x}_p$, which only has K_0 active taps. Given this approach, we can now decompose the original channel measurement as

$$\mathbf{H}[i] = \sum_{p=1}^{P} \mathbf{Q}_p \mathbf{F}\mathbf{x}_p[i], \tag{3}$$

where $\mathbf{Q}_p$ is a diagonal matrix, with

$$Q_{i,i} = \begin{cases} 1 & (p-1)\frac{N}{P} < i \leq p\frac{N}{P} \\ 0 & \text{otherwise} \end{cases} \tag{4}$$

This decomposition results in $\mathbf{Q}_p\mathbf{Q}_q = \mathbf{Q}_p$ iff $p = q$, and the all zeros matrix $\mathbf{0}$ otherwise. Thus, $\mathbf{Q}_p$ are mutually orthogonal projection matrices. Furthermore, $\sum_{p=1}^{P} \mathbf{Q}_p$ equals the identity matrix $\mathbf{I}$.

We now want to find estimates for the P subband delay-lines $\mathbf{x}_p[i]$. Following our assumption on the clustering, these $\mathbf{x}_p[i]$ are expected to be sparse. Thus, we base our approach on the complex LASSO (c-LASSO) algorithm [12], which was used in [13] to estimate sparse tapped delay lines. This algorithm minimizes the Mean Squared Error (MSE) of the channel estimation under the side constraint that exactly K_0 active taps are used. In this case however, we have to consider the full channel estimate according to Equation (3). The LASSO in its Lagrangian form is written as

$$\hat{\mathbf{x}}_1[i], \hat{\mathbf{x}}_2[i], \ldots = \underset{\mathbf{x}_1,\mathbf{x}_2,\ldots}{\operatorname{argmin}} \Big(\Big\| \mathbf{S}\big(\mathbf{H}[i] - \sum_{p=1}^{P} \mathbf{Q}_p \mathbf{F}\mathbf{x}_p\big) \Big\|_2^2 + \sum_{p=1}^{P} \mu_p ||\mathbf{x}_p||_1 \Big). \tag{5}$$

The p-norm is denoted as $\| \cdot \|_p$, and the minimization is conducted jointly with respect to all variables $\mathbf{x}_p$. the P Lagrangian multipliers μ_p tune the 1-norm side constraints on all vectors $\mathbf{x}_p$. This controls the resulting sparseness of the estimates. Matrix $\mathbf{S}$ selects the frequencies of interest. To select the central N_S frequencies, $\mathbf{S}$ is constructed as

$$\mathbf{S} = \operatorname{Diag}\left(\begin{bmatrix} \mathbf{0}^{1\times(N-N_S)/2} & \mathbf{1}^{1\times N_S} & \mathbf{0}^{1\times(N-N_S)/2} \end{bmatrix} \right), \tag{6}$$

where $\operatorname{Diag}(\cdot)$ constructs a diagonal matrix with the given vector as main diagonal. Since the matrices $\mathbf{Q}_p$ are mutually orthogonal subband projection matrices, we are able to exchange the 2-norm and summation operator in Equation (5), resulting in

$$\hat{\mathbf{x}}_1[i], \hat{\mathbf{x}}_2[i], \ldots = \underset{\mathbf{x}_1,\mathbf{x}_2,\ldots}{\operatorname{argmin}} \sum_{p=1}^{P} \Big(\big\| \mathbf{S}\mathbf{Q}_p \left(\mathbf{H}[i] - \mathbf{F}\mathbf{x}_p\right) \big\|_2^2 + \mu_p \big\| \mathbf{x}_p \big\|_1 \Big). \tag{7}$$

Here, each sum term only depends on one minimization variable and its corresponding multiplier, meaning that the optimization problem is decoupled. The sum terms themselves have the same structure now as in [13]. Therefore, the algorithm from Table 3 in [12] can be applied to find the single $\mathbf{x}_p$ individually. This of course means that the overall model, which consists of P delay lines, each of which have a sparsity K_0, has a total model order of $M = K_0 P$. Once the subband impulse responses are estimated, an overall cluster estimate can be computed as

$$\hat{\mathbf{x}}_{\text{cluster}} = \mathbf{F}^{-1} \Big(\sum_{p=1}^{P} \mathbf{Q}_p \mathbf{F} \hat{\mathbf{x}}_p[i] \Big). \tag{8}$$

The results from the algorithm will be compared to the results from *peak search* [13]. In peak search, we first compute the dense impulse response $\mathbf{x}' = \mathbf{F}^H \mathbf{H}$. Then, we establish the delays by finding the M strongest peaks in $\mathbf{x}'$. Finally, we construct the tall DFT matrix $\mathbf{F}' \in \mathbb{C}^{N\times M}$, and compute the peak search estimate through the Moore-Penrose pseudoinverse $(\cdot)^\dagger$ as $\mathbf{x}_{\text{peak}} = (\mathbf{F}')^\dagger \mathbf{H}$.

III. Cluster Fitting Measurement Data

A detailed description of the measurement setup is found in [8].

A. Measurement Setup

In order to understand the measurement data better, we show a photo of the measurement setup in Figure 2. The idea in a nutshell: We keep transmitter (a tripod) and receiver (the silver Mazda) static and let the ordinary street traffic pass. To access to impact of different antenna configuration we measured different overtaking vehicle with different transmit and receive antennas. Our frequency range is 59.75 to 50.25 GHz and Tx and Rx are approximately 18 m apart. Photographs of the used antennas are shown in Figure 3.

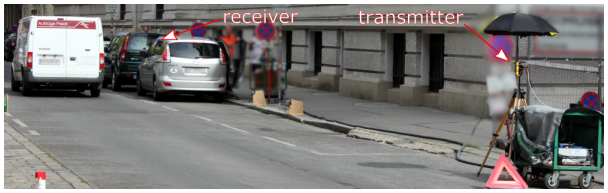

Fig. 2. The measurement site. The transmitter and receiver are static.

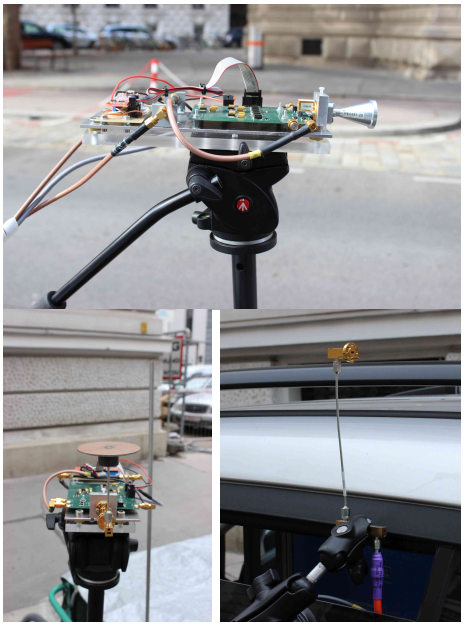

Fig. 3. The antenna types used for the measurement. (top) A 20 dBi horn antenna as transmit antenna. (left) A custom-built quarter wavelength omni-directional antenna as transmit antenna. (right) An open-ended waveguide (OEW) as receive antenna.

We now analyze the cluster-fitting properties based on our measurements. We will first introduce the antenna configurations we choose to analyze, before investigating the cluster fitting performance based on the MSE. Since the measurements have a delay resolution of 2 ns, and light travels 60 cm in 2 ns, we consider cluster sizes of $P = 1$, 2 and 4. This relates to a maximum of 2.4 m multipath length difference that will be compressed in one tap, which is a reasonable assumption for vehicles causing scattering clusters. We present 4 different setups with different antenna types and antenna polarization.

1) Omni-Omni co-polarized: We use 2 omni-directional antennas, both vertically polarized. This measurement serves as a baseline for the other results.

2) Horn-OEW cross-polarized: The transmitter uses a horn antenna with horizontal polarization, while the receiver uses an open-ended waveguide (OEW) with vertical polarization.

3) Horn-Omni co-polarized: The transmitter uses a vertically polarized horn antenna, and the receiver a vertically polarized omni-directional antenna.

4) Horn-Omni cross-polarized: Here, the transmitter uses a horizontally polarized horn, while the receiver uses a vertically polarized omni-directional antenna.

B. Results

Figure 4 shows a sample impulse response for each of the antenna configurations. The time axis is shifted such that the line-of-sight (LOS) path is placed at a relative delay of $\tau = 0$. Additionally, it shows the locations of the nonzero entries for the subband impulse responses $\mathbf{x}_p$ for $P = 4$, with $K_0 = 4$. This was shown to be a good choice for cluster counts in [14]. The noise floor is estimated using the median [15]. Finally, it shows the estimated overall cluster impulse response according to Equation (8). As is shown especially in the Omni-Omni setup, that the algorithm identifies the two strongest components, and assigns them taps in most subband impulse responses. The other tap placements vary but the algorithm avoids putting them all on the strongest tap. Very similar behavior is demonstrated in all the other responses. The estimate does not work well below the estimated noise threshold, but effectively captures the clusters that carry the energy.

The MSE performance of the estimates as a function of the model order M is shown in Figure 5. In this case, the MSE is defined as

$$\text{MSE} = \frac{||\mathbf{S}(\mathbf{H}-\mathbf{F}\mathbf{x})||_2^2}{N_S}, \tag{9}$$

and the model order $M = P \cdot K_0$. This normalization ensures that we are comparing models with the same total number of degrees of freedom. Here, we see that the cross-polarized measurement fits have higher MSEs. This is caused by the multipaths being much stronger relative to the LOS path, and thus the channel appearing less sparse. Furthermore, in two of the 4 constellations, peak search is not monotonically decreasing. This is caused by the projection to $\mathbf{S}$, which disregards some subcarriers. As it happens, sometimes peak search with $M = 5$ mostly improves the out-of-band performance.

The LASSO algorithm can be seen to not converge well with $P = 1$. However, the fit with $P = 2$ already performs well, and $P = 4$ outperforms peak search 3 of the 4 cases. The only exception here is the Omni-Omni configuration, but even there it is not worse. The

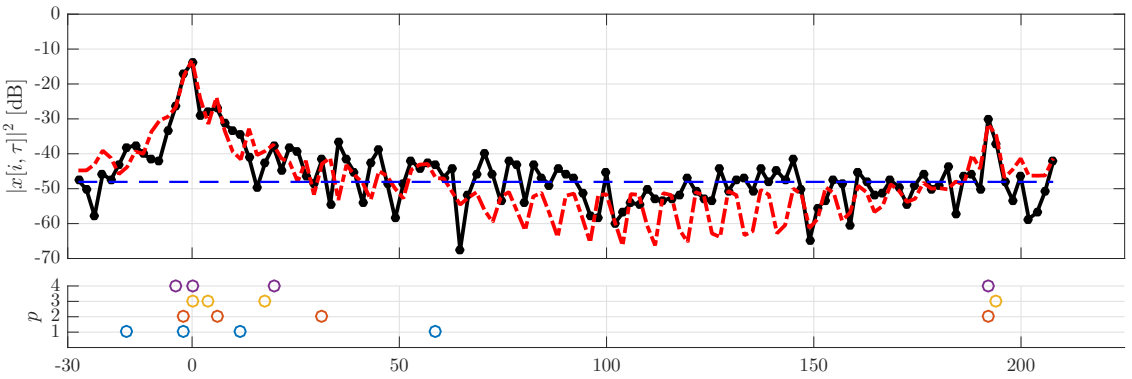

(a) Omni-Omni co-polarized

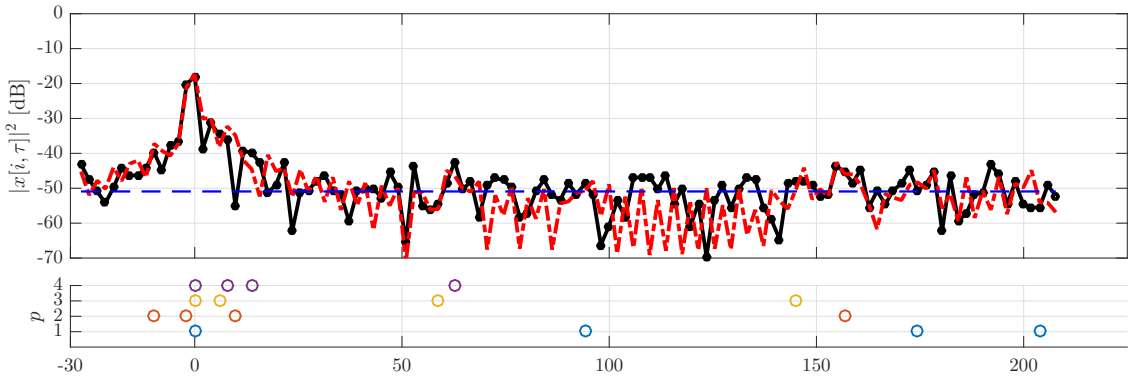

(b) Horn-OEW cross-polarized

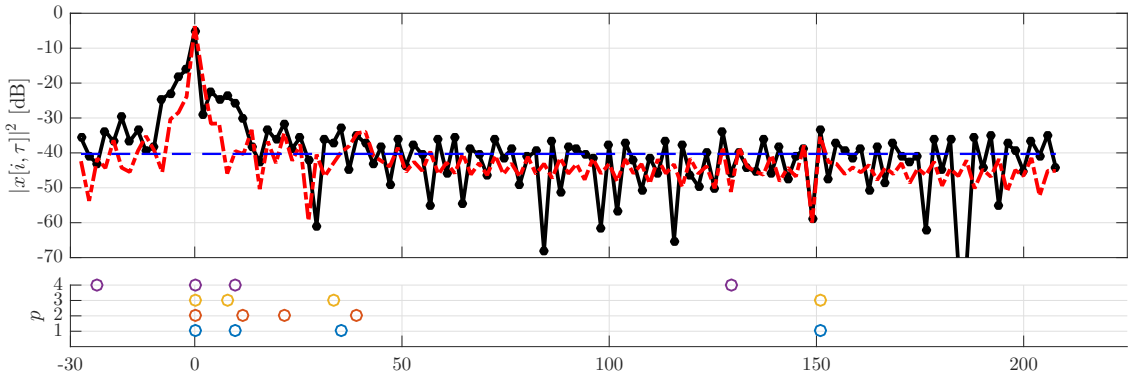

(c) Horn-Omni co-polarzied

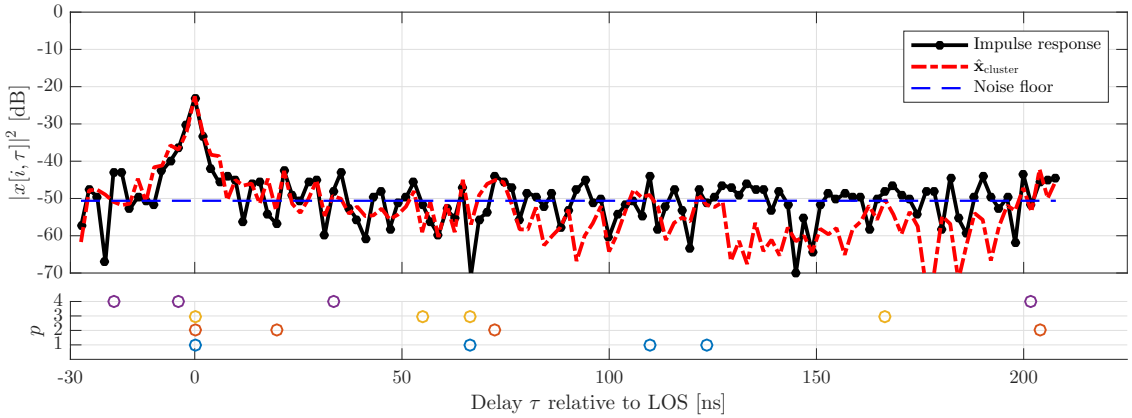

(d) Horn-Omni cross-polarized

Fig. 4. Sample impulse responses, estimated cluster impulse responses and cluster locations for $P = 4$, $K_0 = 4$ fits.

biggest achievable gain can be found in the Horn-Omni co-polarized scenario, where both $P = 2$ and $P = 4$ fits outperform peak search by a large margin.

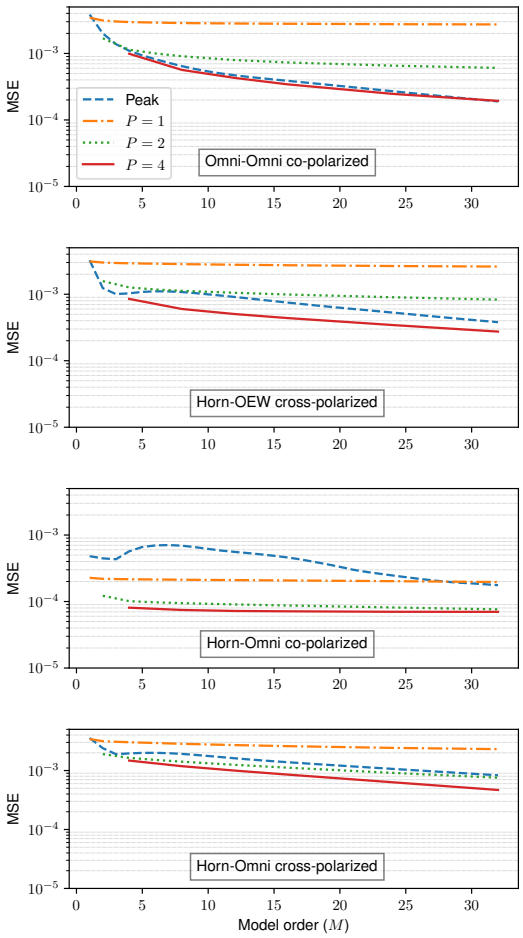

Fig. 5. MSEs for cluster fitting of the 4 measurement setups.

IV. Conclusions

We demonstrate a sparse analysis of mmWave vehicular channels. Our results show that the measurements exhibit a cluster structure in the channel, that is well exploited using subband cluster fitting. The higher the partition order P was chosen, the better the LASSO algorithm was able to converge. Our results confirm that in mmWave communications, the antenna choices are inseparable from the channel, but in all cases, we are able to find a suitable sparse fit. This result is of high interest, as it shows that parallel subband descriptions are a good modeling approach for the investigated channel, and instead of losing degrees of freedom, exploit the observed structure.

Acknowledgements

The financial support by the Austrian Federal Ministry of Science, Research and Economy and the National Foundation for Research, Technology and Development is gratefully acknowledged. The research has been co-financed by the Czech Science Foundation, Project No. 17-18675S "Future transceiver techniques for the society in motion", and by the Czech Ministry of Education in the frame of the National Sustainability Program under grant LO1401.This work was partially funded by Austrian Development Cooperation and Ministry of Education, Science and Technology of Republic of Kosovo, in the framework of the project HERAS K-01-2017 as research cooperation and networking between Austria, Kosovo and the Western Balkan Region.

References

[1] J. Choi, V. Va, N. Gonzalez-Prelcic, R. Daniels, C. R. Bhat, and R. W. Heath, "Millimeter-wave vehicular communication to support massive automotive sensing," *IEEE Communications Magazine*, vol. 54, no. 12, pp. 160–167, December 2016.

[2] C. F. Mecklenbräuker, A. F. Molisch, J. Karedal, F. Tufvesson, A. Paier, L. Bernado, T. Zemen, O. Klemp, and N. Czink, "Vehicular Channel Characterization and Its Implications for Wireless System Design and Performance," *Proc. IEEE*, vol. 99, no. 7, pp. 1189–1212, Jul 2011.

[3] T. S. Rappaport, G. R. MacCartney, M. K. Samimi, and S. Sun, "Wideband millimeter-wave propagation measurements and channel models for future wireless communication system design," *IEEE Trans. on Communications*, vol. 63, no. 9, pp. 3029–3056, Sept 2015.

[4] E. Zöchmann *et al.*, "Directional evaluation of receive power, Rician K-factor and RMS delay spread obtained from power measurements of 60 GHz indoor channels," in *Proc. of IEEE-APS Topical Conference on Antennas and Propagation in Wireless Communications (APWC)*, 2016, pp. 246–249.

[5] E. Zöchmann, M. Lerch, S. Pratschner, R. Nissel, S. Caban, and M. Rupp, "Associating spatial information to directional millimeter wave channel measurements," in *Proc. of IEEE 86th Vehicular Technology Conference (VTC-Fall)*, 2017.

[6] E. Ben-Dor, T. S. Rappaport, Y. Qiao, and S. J. Lauffenburger, "Millimeter-wave 60 GHz outdoor and vehicle AOA propagation measurements using a broadband channel sounder," in *Proc. 2011 IEEE GLOBECOM*, Dec 2011, pp. 1–6.

[7] J. Blumenstein, A. Prokes, A. Chandra, T. Mikulasek, R. Marsalek, T. Zemen, and C. Mecklenbräuker, "In-vehicle channel measurement, characterization, and spatial consistency comparison of 3-11 GHz and 55-65 GHz frequency bands," *IEEE Trans. on Veh. Techn.*, vol. 66, no. 5, pp. 3526–3537, 2017.

[8] E. Zöchmann *et al.*, "Measured delay and Doppler profiles of overtaking vehicles at 60 GHz," in *Proc. of the 12th European Conference on Antennas and Propagation (EuCAP)*, 2018.

[9] A. A. M. Saleh and R. Valenzuela, "A statistical model for indoor multipath propagation," *IEEE Journal on Selected Areas in Communications*, vol. 5, no. 2, pp. 128–137, Feb 1987.

[10] C. Gustafson, K. Haneda, S. Wyne, and F. Tufvesson, "On mm-Wave multipath clustering and channel modeling," *IEEE Transactions on Antennas and Propagation*, vol. 62, no. 3, pp. 1445–1455, Mar 2014.

[11] R. He, W. Chen, B. Ai, A. F. Molisch, W. Wang, Z. Zhong, J. Yu, and S. Sangodoyin, "On the clustering of radio channel impulse responses using sparsity-based methods," *IEEE Trans. on Antennas and Propagation*, vol. 64, no. 6, pp. 2465–2474, June 2016.

[12] C. F. Mecklenbräuker, P. Gerstoft, and E. Zöchmann, "c–LASSO and its dual for sparse signal estimation from array data," *Signal Processing*, vol. 130, pp. 204–216, 2017.

[13] T. Blazek and C. Mecklenbräuker, "Sparse time-variant impulse response estimation for vehicular channels using the c-LASSO," in *Proc. 2017 IEEE PIMRC*, Oct 2017.

[14] T. Blazek, E. Zöchmann, and C. Mecklenbräuker, "Model order selection for LASSO fitted millimeter wave vehicular channel data," in *Proc. 2018 IEEE 29th PIMRC*, Sep. 2018.

[15] E. S. Sousa, V. M. Jovanovic, and C. Daigneault, "Delay spread measurements for the digital cellular channel in Toronto," *IEEE Transactions on Vehicular Technology*, vol. 43, no. 4, pp. 837–847, 1994.